JCI insight

RESEARCH ARTICLE

Extrapulmonary *Aspergillus* infection in patients with CARD9 deficiency

Nikolaus Rieber,[1,2] Roel P. Gazendam,[3] Alexandra F. Freeman,[4] Amy P. Hsu,[4] Amanda L. Collar,[4] Janyce A. Sugui,[4] Rebecca A. Drummond,[4] Chokechai Rongkavilit,[5] Kevin Hoffman,[6] Carolyn Henderson,[4] Lily Clark,[4] Markus Mezger,[1] Muthulekha Swamydas,[4] Maik Engeholm,[7] Rebecca Schüle,[7] Bettina Neumayer,[8] Frank Ebel,[9] Constantinos M. Mikelis,[10] Stefania Pittaluga,[11] Vinod K. Prasad,[12] Anurag Singh,[1] Joshua D. Milner,[13] Kelli W. Williams,[4] Jean K. Lim,[5] Kyung J. Kwon-Chung,[4] Steven M. Holland,[4] Dominik Hartl,[1] Taco W. Kuijpers,[3] and Michail S. Lionakis[4]

[1]Infectious Diseases and Immunology, Department of Pediatrics I, University of Tübingen, Germany. [2]Department of Pediatrics, Munich Schwabing Hospital, Munich Technical University, Munich, Germany. [3]Sanquin Research, and Landsteiner Laboratory, Academic Medical Center, University of Amsterdam, Amsterdam, The Netherlands. [4]Laboratory of Clinical Infectious Diseases, National Institute of Allergy and Infectious Diseases (NIAID), National Institutes of Health (NIH), Bethesda, Maryland, USA. [5]Wayne State University and Children's Hospital of Michigan, Detroit, Michigan, USA. [6]Department of Microbiology, Icahn School of Medicine at Mount Sinai, New York, New York, USA. [7]Department of Neurodegenerative Disease, Hertie-Institute for Clinical Brain Research and Center for Neurology, Tübingen, Germany. [8]Institute of Pathology, University of Tübingen, Tübingen, Germany. [9]Max-von-Pettenkofer-Institute, Ludwig-Maximilians-University, Munich, Germany. [10]Department of Biomedical Sciences, School of Pharmacy, Texas Tech University Health Sciences Center, Amarillo, Texas, USA. [11]Center for Cancer Research, National Cancer Institute, NIH, Bethesda, Maryland, USA. [12]Pediatric Blood and Marrow Transplantation, Duke University Medical Center, Durham, North Carolina, USA. [13]Laboratory of Allergic Diseases, NIAID, NIH, Bethesda, Maryland, USA.

Invasive pulmonary aspergillosis is a life-threatening mycosis that only affects patients with immunosuppression, chemotherapy-induced neutropenia, transplantation, or congenital immunodeficiency. We studied the clinical, genetic, histological, and immunological features of 2 unrelated patients without known immunodeficiency who developed extrapulmonary invasive aspergillosis at the ages of 8 and 18. One patient died at age 12 with progressive intra-abdominal aspergillosis. The other patient had presented with intra-abdominal candidiasis at age 9, and developed central nervous system aspergillosis at age 18 and intra-abdominal aspergillosis at age 25. Neither patient developed *Aspergillus* infection of the lungs. One patient had homozygous M1I *CARD9* (caspase recruitment domain family member 9) mutation, while the other had homozygous Q295X *CARD9* mutation; both patients lacked CARD9 protein expression. The patients had normal monocyte and Th17 cell numbers in peripheral blood, but their mononuclear cells exhibited impaired production of proinflammatory cytokines upon fungus-specific stimulation. Neutrophil phagocytosis, killing, and oxidative burst against *Aspergillus fumigatus* were intact, but neither patient accumulated neutrophils in infected tissue despite normal neutrophil numbers in peripheral blood. The neutrophil tissue accumulation defect was not caused by defective neutrophil-intrinsic chemotaxis, indicating that production of neutrophil chemoattractants in extrapulmonary tissue is impaired in CARD9 deficiency. Taken together, our results show that CARD9 deficiency is the first known inherited or acquired condition that predisposes to extrapulmonary *Aspergillus* infection with sparing of the lungs, associated with impaired neutrophil recruitment to the site of infection.

Authorship note: N. Rieber, R.P. Gazendam, and A.F. Freeman all contributed equally to this work. D. Hartl, T.W. Kuijpers, and M.S. Lionakis all contributed equally to this work.

Conflict of interest: The authors declare that no conflict of interest exists.

Submitted: August 1, 2016
Accepted: September 16, 2016
Published: October 20, 2016

Reference information:
JCI Insight. 2016;1(17):e89890.
doi:10.1172/jci.insight.89890.

Introduction

Invasive pulmonary infections by the ubiquitous inhaled mold *Aspergillus* are an emerging problem in patients with iatrogenic immunosuppression during chemotherapy-induced neutropenia, corticosteroids, and/or hematopoietic stem cell transplantation (1–3). Invasive aspergillosis in primary immunodeficiencies is rare, and largely limited to pulmonary disease in chronic granulomatous disease (CGD) and GATA binding protein 2 (GATA2) deficiency (3–5).

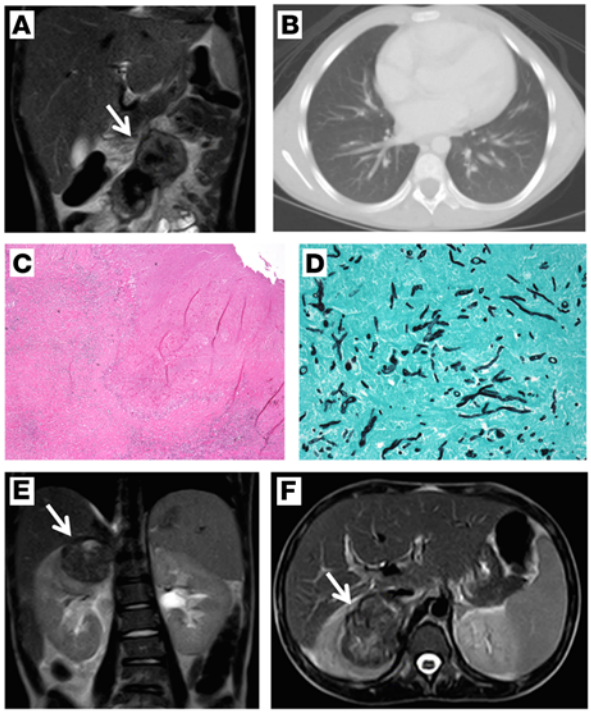

Figure 1. Intra-abdominal aspergillosis in CARD9 (caspase recruitment domain family member 9) deficiency. Coronal image of computed tomography of the abdomen of patient 2 shows a large intra-abdominal mass (**A**, arrow), while chest computed tomography shows normal lungs (**B**). Biopsy of the intra-abdominal mass shows areas of palisading inflammation and necrosis on H&E stain (**C**; magnification, ×40) and acute-angle branching hyphae consistent with *Aspergillus* species on Grocott-Gomori's methenamine silver stain (**D**; magnification, ×400). Coronal (**E**) and axial (**F**) images of computed tomography of the abdomen of patient 2 one year after the initial presentation shows a large right suprarenal mass (arrows).

Mutations in fungal pattern recognition receptor (PRR) and downstream signaling pathway genes have not yet been associated with Mendelian susceptibility to aspergillosis (6). Fungi are recognized via PRRs, particularly C-type-lectin receptors (CLRs), Toll-like receptors (TLRs), and complement receptor 3 (CR3) (7–9). TLR signaling appears redundant for human antifungal host defense, as patients with myeloid differentiation primary response 88 (*MYD88*) and interleukin-1 receptor-associated kinase 4 (*IRAK4*) mutations develop pyogenic bacterial but not fungal infections (10). Mouse and in vitro studies have shown that CLRs including dectin-1, dectin-2, dectin-3, and mincle, and their downstream adaptor CARD9 play a pivotal role in fungal sensing (7, 8, 11). The relevance of this pathway in humans was shown by several cases of CARD9 deficiency in families with chronic mucocutaneous candidiasis (CMC) and invasive candidiasis of the intestine and central nervous system (CNS) (12–14). The spectrum of fungal disease in human CARD9 deficiency was recently expanded to include superficial and deep dermatophytosis as well as subcutaneous and invasive phaeohyphomycosis (15–17). At the mechanistic level, mouse and human CARD9 deficiency have been associated with decreased peripheral Th17 cells (12), impaired production of proinflammatory cytokines upon fungus-specific stimulation (13, 14, 18, 19), impaired phagocyte killing of unopsonized yeasts (14, 19), and defective generation of myeloid-derived suppressor cells (20), some of which may contribute to heightened susceptibility to fungal disease. However, infections by ubiquitous inhaled *Aspergillus* have not been reported in CARD9-deficient patients thus far.

Here, we describe 2 unrelated patients with different homozygous *CARD9*-null mutations who had invasive CNS and intra-abdominal aspergillosis, while, strikingly, their lungs were spared from the infection. We uncover a role for CARD9 in promoting neutrophil accumulation in *Aspergillus*-infected extrapulmonary tissues, whereas neutrophil-intrinsic chemotaxis and anti-*Aspergillus* effector functions are CARD9 independent.

Results

Case descriptions

Patient 1. A 9-year-old male of mixed European descent born to healthy consanguineous parents, manifested chronic oral candidiasis, followed by intra-abdominal candidiasis of the liver and mesenteric lymph nodes that was successfully treated with amphotericin B. At age 18, biopsy of cerebral lesions in the thalamus and capsula interna revealed acute-angle branching septate hyphae, most consistent with the diagnosis of cerebral aspergillosis. The infection responded to surgical resection and amphotericin B. At age 25, biopsy of hepatic and mesenteric lymph node lesions showed acute-angle branching septate hyphae, most consistent with the diagnosis of aspergillosis. Chest computed tomography showed no lung involvement. The infection resolved with itraconazole; secondary prophylaxis has continued for 20 years without recurrence. The patient did not have severe or recurrent bacterial or viral infections, but had autosomal dominant hereditary spastic paraplegia due to a *SPAST* (Spastin) mutation (21).

Besides mild lymphopenia (700–1,000 lymphocytes/μl), immunological evaluations were within normal age ranges, including neutrophil and monocyte numbers in peripheral blood, percentages of lymphocyte subsets, T cell functions, and humoral immune parameters (Tables 1 and 2). Due to spastic paraplegia and lymphopenia, defects in adenosine deaminase and purine nucleoside phosphorylase activity were biochemically excluded. CGD and HIV infection were ruled out by laboratory testing.

Table 1. Lymphocyte immunophenotyping parameters in the peripheral blood of the caspase recruitment domain family member 9 (CARD9)-deficient patients of this study

Immunophenotyping parameter	Patient 1 % (absolute)	Patient 2 % (absolute)	Normal %	Normal absolute (cells/μl)
Lymphocytes				
T Lymphocytes	63 (450)	63.4 (2,162)	55–83	700–2,100
$CD4^+$ T cells	42 (300)	27.6 (941)	28–57	300–1,400
$CD8^+$ T cells	19 (136)	31.4 (1,071)	10–39	200–900
B Lymphocytes	24 (171)	25.3 (863)	6–19	100–500
NK cells	13 (93)	10.8 (368)	7–31	90–600
T Lymphocytes				
$CD45RA^+$	23 (59)	ND	3–59	27–833
$CD45RO^+$	73 (188)	ND	15–69	167–670
$CD45RA^+CD31^+$	17 (48)	ND	6–42	42–399
Th17[A]	1.94	3.95	0.2–3.5	
B Lymphocytes				
$CD27^+$	25 (36)	ND	6–53	18–145
$CD27^+IgM^+IgD^+$	15 (21)	ND	2–29	4–85
$CD27^+IgM^-IgD^-$	8 (11)	ND	2–27	7–61

[A]Th17 numbers represent % of cells within CD4+ T cells. ND, not determined

Patient 2. A 12-year-old African-American boy, presented at 8 years with a 5-month history of weight loss, fever, and abdominal pain. An abdominal mass encasing the celiac, mesenteric, and renal arteries measured 7.5 × 9 cm (Figure 1A). Chest computed tomography was unremarkable (Figure 1B). An open biopsy showed necrotizing granulomatous inflammation and acute-angle branching septate hyphae (Figure 1, C and D), and grew *Aspergillus fumigatus*. One year later, a new suprarenal mass (Figure 1, E and F) developed with histology and culture confirming *A. fumigatus* invasive infection. Over the next 3 years, the infection progressed despite aggressive antifungal drug therapy. He underwent surgical debulking of the intra-abdominal masses followed by double-cord stem cell transplantation; transplant was complicated by failure to engraft. Repeat double-cord stem cell transplantation 8 weeks later was complicated by hepatic veno-occlusive disease and fatal diffuse alveolar hemorrhage.

The patient had tinea corporis before aspergillosis but no CMC, CNS candidiasis, severe or recurrent bacterial or viral infections. He had mild eczema, food allergies, and reactive airway disease. He had normal numbers of neutrophils, monocytes, and lymphocytes in peripheral blood and intermittently elevated eosinophils (range, 400–1,000 cells/μl). He had normal tests for CGD, normal immunoglobulin levels except for elevated IgE (range, 600–1,100 IU/ml), and normal lymphocyte phenotyping (Tables 1 and 2).

Biallelic *CARD9* mutations in the patients with extrapulmonary aspergillosis

In search of a monogenic cause for the susceptibility to aspergillosis, different strategies were employed in the 2 patients. Whole-exome sequencing (WES) of patient 1 yielded a previously reported homozygous *CARD9* mutation (c.883C>T), resulting in a premature termination codon (p.Q295X) with absent protein (Figure 2A) (12). The mutation was confirmed by Sanger sequencing and RFLP (Supplemental Figure 1, A and B; supplemental material available online with this article; doi:10.1172/jci.insight.89890DS1). No other mutations

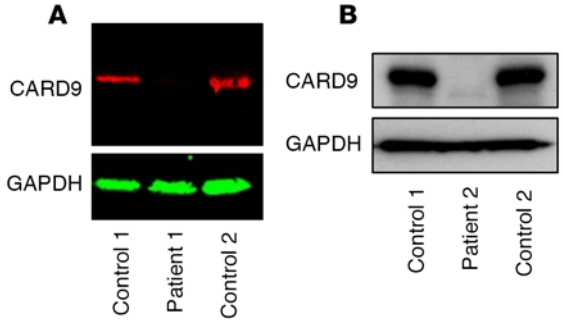

Figure 2. The patients with extrapulmonary aspergillosis carry biallelic caspase recruitment domain family member 9 (*CARD9*) mutations that result in absent CARD9 protein. Western blots of CARD9 protein expression in peripheral blood mononuclear cells from healthy donors and patient 1 (left panel) and 2 (right panel). GAPDH is shown as a loading control.

Table 2. Immunological parameters of the caspase recruitment domain family member 9 (CARD9)-deficient patients of this study

Lymphocyte Proliferation	Patient 1	Patient 2	Humoral response	Patient 1	Patient 2	Normal
Mitogens			**Total IgG**	11.4 g/l	21.0	7–16 g/l
PHA	Normal	ND				
OKT3	Normal	ND	**Specific antibody titers**			
Con A	Normal	ND	Tetanus	Present	Present	
PWM	Normal	ND	Diphtheria	Present	Present	
SAC	Normal	ND	*Hemophilus*	Present	Present	
			Pneumococcus	Present	Present	
Antigens			**IgE**	ND	828	IU/mL
Tetanus/Diphtheria/ Streptolysin O/Mumps	Normal	ND				

ND, not determined; PHA, phytohemagglutinin; OKT3, monoclonal anti-CD3 antibody; Con A, concanavalin A; PWM, pokeweed mitogen; SAC, *Staphylococcus aureus* Cowan I.

in known primary immunodeficiency disorder genes, including those associated with invasive mold disease (*GATA2* and signal transducer and activator of transcription 1 [*STAT1*]) (4) were identified via WES. In patient 2, targeted *CARD9* sequencing revealed a homozygous mutation in the start codon, c.3G>C, p.M1I (Supplemental Figure 1C) that resulted in absent protein (Figure 2B). The c.883C>T mutation has previously been reported to be rare, as it was not found in the 1000 Genomes, HGMD, or Ensembl databases (13), and has a population frequency of 3.03×10^{-5} in ExAC, being identified in a heterozygous state in 3 individuals out of 98,954 alleles, 1 each being Latino, South Asian, and Other. In addition, as previously reported (13), it is predicted to be deleterious by CADD (PHRED score, 37), and pathogenic by ClinVar. The c.3G>C mutation was not found in the 1000 Genomes, NHLBI6500, or ExAC databases, covering 118,000 chromosomes in the specific exon, and was predicted to be deleterious by CADD (PHRED score, 22.1) and PolyPhen 2 (score, 0.924) (22, 23). Targeted sequencing of *GATA2* and *STAT1* in patient 2 revealed no mutations.

CARD9 c.883C>T and c.3G>C impair fungus-stimulated cytokine production

We first sought to examine the functional consequences of the patients' mutations by measuring the production of proinflammatory cytokines from peripheral blood mononuclear cells (PBMCs) induced with fungal (*Candida albicans*, *A. fumigatus*) or nonfungal (LPS, *Staphylococcus aureus*) stimuli. Consistent with previously reported *CARD9* mutations (12–14, 19, 24), the patient cells produced decreased IL-1β, IL-6, TNF-α, and GM-CSF after stimulation with *C. albicans*, while cytokine production was normal following LPS or *S. aureus* stimulation (Figure 3). CARD9-deficient PBMCs also produced less TNF-α, GM-CSF, and IFN-γ following stimulation with heat-killed *A. fumigatus* conidia (Figure 4). Decreased proportions of $IL\text{-}17^{+}CD4^{+}$ T cells in peripheral blood have been reported in some, but not all, CARD9-deficient patients (12–15, 17, 25). IL-17A production by our patients' $CD4^{+}$ T cells was intact (Table 1). This finding is consistent with the dispensable role of IL-17 signaling in anti-*Aspergillus* host defense in humans with mutations in *IL17RA*, *IL17F*, *IL17RC*, and *ACT1* (6).

CARD9 deficiency does not impair the anti-*Aspergillus* effector function of human neutrophils

Because neutrophils are the principal cells that mediate anti-*Aspergillus* host defense (26), we examined neutrophil effector function against *A. fumigatus* conidia and hyphae, the 2 developmental stages of fungal growth; conidia are the inhaled infectious particles, which germinate into hyphae that invade through the infected tissue in profoundly immunosuppressed patients (1, 27). Notably, CARD9-deficient neutrophils exhibited normal capacity to internalize conidia (Figure 5), to prevent conidial germination to hyphae (Supplemental Figure 2), and to kill opsonized or unopsonized conidia and hyphae (Figure 5), in agreement with intact anti-*Aspergillus* killing of $Card9^{-/-}$ mouse neutrophils (28). Furthermore, CARD9-deficient neutrophils had normal oxidative burst towards fungal and nonfungal stimuli ex vivo (Supplemental Figure 3), and exerted oxidative cytotoxicity on the B-5233/GFP *Aspergillus* strain that expresses GFP during oxidative stress (Supplemental Figure 3). Together, these data show that CARD9 is dispensable for anti-*Aspergillus* effector function in human neutrophils. Of note, these findings contrast with the previously reported selec-

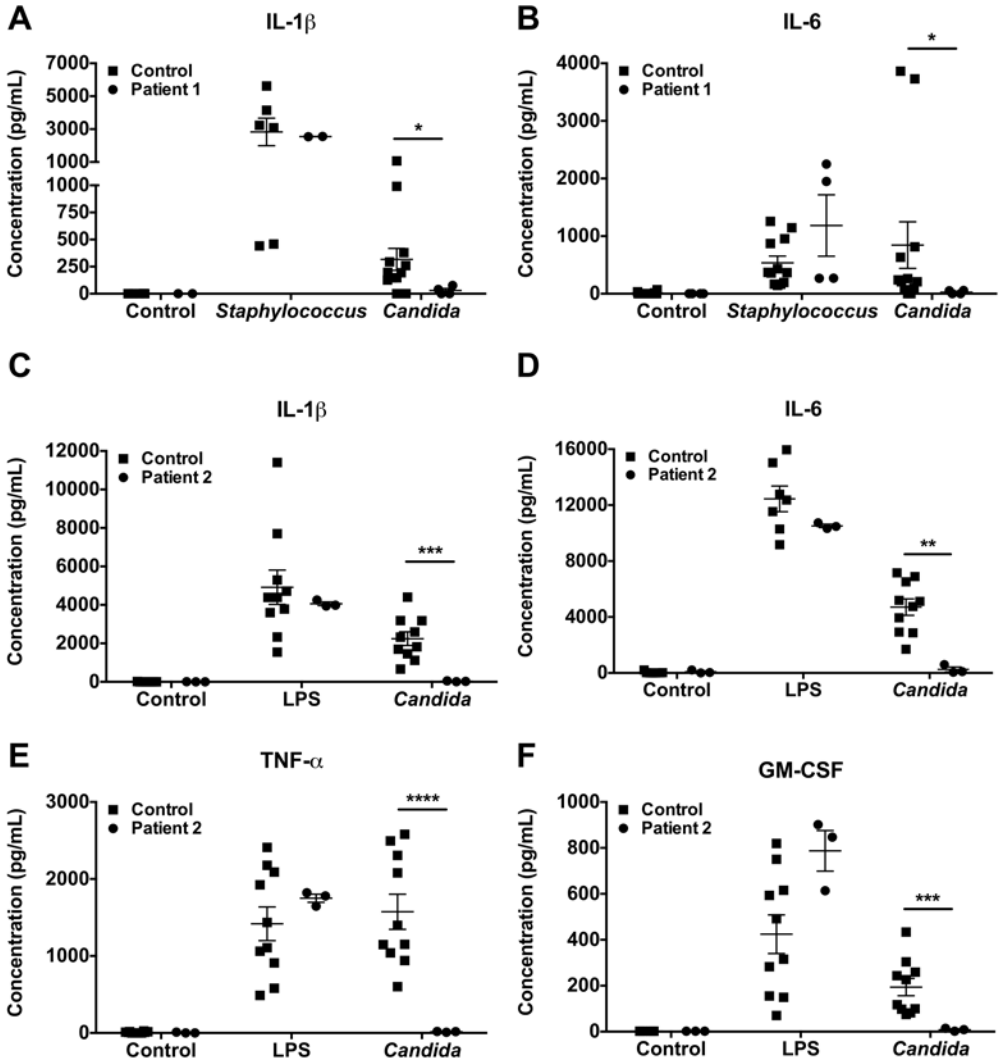

Figure 3. Caspase recruitment domain family member 9 (CARD9) deficiency results in impaired production of proinflammatory mediators upon fungal-specific stimulation. IL-1β (**A**; $^{*}P = 0.0275$, Mann-Whitney test) and IL-6 (**B**; $^{*}P = 0.0275$, Mann-Whitney test) production by healthy donor ($n = 6–12$) and patient 1 ($n = 2–4$ independent experiments) peripheral blood mononuclear cells (PBMCs) after 24 hours of stimulation with live *Candida albicans* or *Staphylococcus aureus* or after 24 hours without stimulation. IL-1β (**C**; $^{***}P = 0.0002$, unpaired *t* test), IL-6 (**D**; $^{**}P = 0.0019$, unpaired *t* test), TNF-α (**E**; $^{****}P < 0.0001$, unpaired *t* test) and GM-CSF (**F**; $^{***}P = 0.0008$, unpaired *t* test) production by healthy donor ($n = 7–10$) and patient 2 ($n = 3$ independent experiments) PBMCs after 48 hours of stimulation with heat-killed *C. albicans* or LPS or after 48 hours without stimulation. Data represent the mean ± SEM.

tive defect of CARD9-deficient neutrophils in killing of unopsonized forms of *Candida*, and indicate that CARD9 exerts differential fungus-specific roles on the effector function of human neutrophils (14, 19, 29).

CARD9 deficiency is associated with impaired neutrophil accumulation in *Aspergillus*-infected tissue

While CARD9-deficient neutrophil anti-*Aspergillus* effector function was unaffected, we observed a striking lack of neutrophils in the *Aspergillus*-infected tissue of patient 2 (Figure 6). We observed necrotic foci with granulomatous inflammation and palisading $CD68^{+}$ histiocytes, which engulfed hyphae (Figure 6, A and B and inset), and surrounding plasma cells and eosinophils (Figure 6, C and D). Similar necrosis without neutrophil infiltration was seen in the infected mesenteric lymph node of patient 1 (Supplemental Figure 4). Because aspergillosis in nonneutropenic mice and humans is accompanied by robust neutrophilic tissue accumulation (28, 30, 31), the lack of tissue neutrophil infiltration in CARD9 deficiency despite normal peripheral neutrophil numbers represents a suboptimal innate

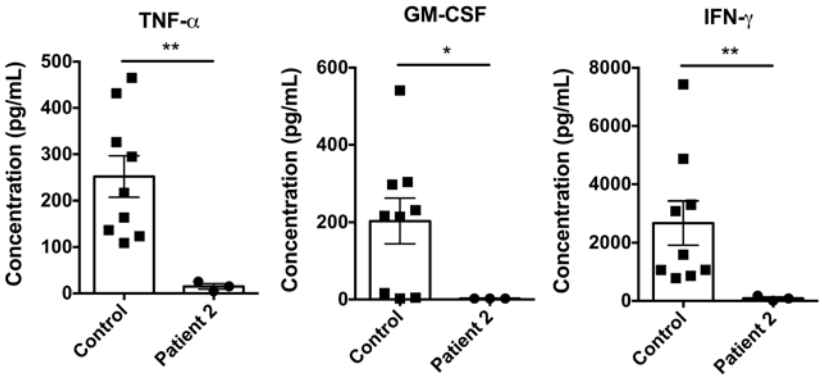

Figure 4. The c.3G>C caspase recruitment domain family member 9 (*CARD9*) loss-of-function mutation impairs the production of proinflammatory mediators upon stimulation with *Aspergillus fumigatus* conidia. TNF-α (**P = 0.0091, Mann-Whitney test), GM-CSF (*P = 0.0273, Mann-Whitney test), and IFN-γ (**P = 0.0091, Mann-Whitney test) production by healthy donor (n = 9) and patient 2 (n = 3 independent experiments) peripheral blood mononuclear cells after 48 hours of stimulation with heat-killed *A. fumigatus* conidia. Data represent the mean ± SEM.

immune response and is consistent with a defect in neutrophil recruitment from the blood into the *Aspergillus*-infected tissue.

Decreased trafficking of neutrophils from the blood into the *Aspergillus*-infected tissue could be explained by the net effect of (a) impaired neutrophil-intrinsic capacity for chemotaxis, and (b) impaired production of neutrophil chemoattractants in the infected extrapulmonary tissue that is essential to create the chemoattractant concentration gradient required for effective cell recruitment. Because it was not possible to directly examine chemoattractant production by human cells from extrapulmonary infected tissues, we focused on determining whether neutrophil-intrinsic chemotaxis is impaired in CARD9-deficient neutrophils. We found normal chemotactic capacity of neutrophils from patient 1 and another patient with the p.Q295X *CARD9* mutation toward IL-8, the complement factor C5a, and platelet-activating factor (PAF) (Supplemental Figure 5), 3 major neutrophil chemoattractant molecules. This finding is consistent with similar results recently reported for neutrophils from a CARD9-deficient patient carrying the missense p.R57H mutation (14). Therefore, extrapulmonary aspergillosis during CARD9 deficiency is associated with an inability to mobilize neutrophils to the site of infection without neutrophil-intrinsic defects in chemotaxis.

Discussion

Herein, we reveal a role for CARD9 in host defense against invasive aspergillosis, expanding the clinical spectrum of CARD9 deficiency beyond CMC, invasive candidiasis, dermatophytosis, and phaeohyphomycosis (13–17, 29, 32). Uniquely, *Aspergillus* in CARD9 deficiency appears to have a predilection for nonpulmonary sites with sparing of the lungs, in contrast with all other known iatrogenic or inherited conditions that cause aspergillosis. Importantly, CARD9 deficiency is associated with impaired neutrophil accumulation at the site of extrapulmonary *Aspergillus* infection, while neutrophil anti-*Aspergillus* effector function is intact.

The extrapulmonary tropism of aspergillosis in our CARD9-deficient patients suggests that inhalation of airborne conidia may lead to inapparent pulmonary aspergillosis followed by disseminated aspergillosis complicated by an inability to mount appropriate immune responses at extrapulmonary sites. The absence of pulmonary *Aspergillus* involvement in CARD9 deficiency may be explained by lung-specific, CARD9-independent immune mechanisms that may compensate for lack of CLR/CARD9 signaling. Indeed, recent mouse studies showed that Card9 plays only a partial role in neutrophil pulmonary recruitment after *Aspergillus* challenge, being compensated by mononuclear phagocyte and epithelial cell IL-1α and Myd88 signaling (28, 33). Thus, CARD9 appears to mediate organ-specific effects on neutrophil recruitment during aspergillosis, being largely redundant for pulmonary recruitment (28) but necessary for recruitment into extrapulmonary organs (current study), in agreement with its CNS-specific role in mediating neutrophil recruitment during systemic candidiasis (14). Because CARD9 is dispensable for neutrophil-intrinsic chemotaxis, CARD9 likely mediates extrapulmonary organ-specific neutrophil recruitment during *Aspergillus* infection via orchestrating the production of neutrophil-targeted chemoattractants in a tissue-specific manner.

Because it was not feasible to directly examine the chemoattractant production potential of extrapulmonary tissue cells in our patients, future studies using *Aspergillus*-infected *Card9*$^{-/-}$ mice and CARD9-null induced pluripotent stem cell–derived (iPSC-derived) cells will be needed to investigate the tissue-specific defects in neutrophil-targeted chemoattractant molecules that may account for the impaired neutrophil accu-

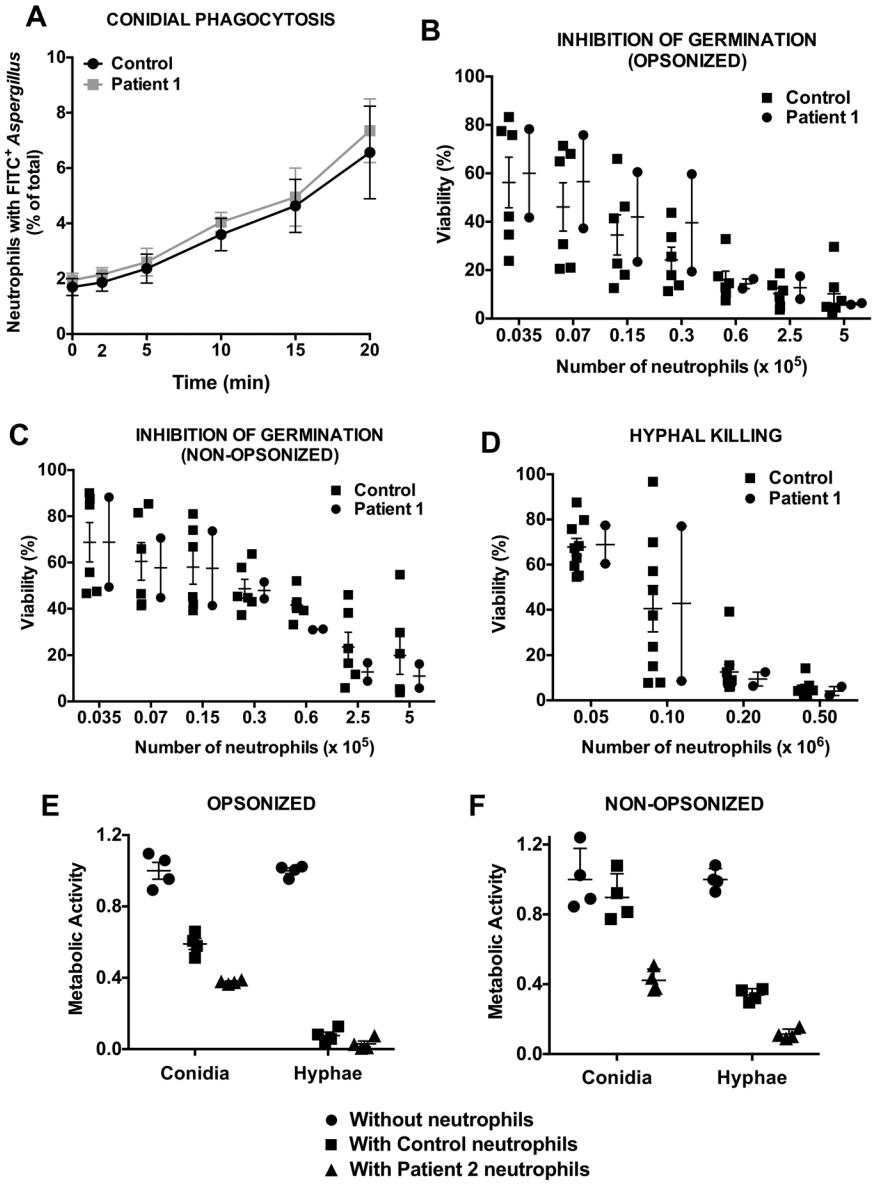

Figure 5. Caspase recruitment domain family member 9 (CARD9) deficiency does not impair neutrophil phagocytosis and killing of *Aspergillus fumigatus*. (**A**) CARD9-deficient neutrophils from patient 1 exhibit normal conidial internalization as assessed by flow cytometry using FITC-labeled *A. fumigatus* conidia (n = 3 healthy donors; n = 2 independent experiments with patient 1 cells). (**B** and **C**) Control neutrophils and CARD9-deficient neutrophils from patient 1 have similar capacity to prevent the germination of opsonized (**B**) and nonopsonized (**C**) *A. fumigatus* conidia into hyphae. Fungal metabolic activity was measured using the MTT assay (n = 6 healthy donors; n = 2 independent experiments with patient 1 cells). (**D**) Killing of opsonized *A. fumigatus* hyphae by control neutrophils and CARD9-deficient neutrophils from patient 1. Fungal metabolic activity was measured using the MTT assay (n = 9 healthy donors; n = 2 independent experiments with patient 1 cells). (**E** and **F**) Opsonized (**E**) and nonopsonized (**F**) conidia or hyphae were incubated with neutrophils (ratio 1:1) from either healthy donors or Patient 2. Fungal metabolic activity was measured using the XTT (2,3-bis-(2-methoxy-4-nitro-5-sulfophenyl)-2H-tetrazolium-5-carboxanilide) assay (n = 4 healthy donors; n = 4 independent experiments with patient 2 cells). Data shown represent 1 of 3 independent replicates with similar patterns of results. Data represent the mean ± SEM (**A**–**D**) or mean ± SD (**E** and **F**).

mulation during extrapulmonary *Aspergillus* infection. In addition, because monocytes and macrophages also play significant roles in anti-*Aspergillus* protective immune responses in mice (26) and may compensate for the lack of neutrophils in patients with congenital neutropenia syndromes, who occasionally but not uniformly suffer from invasive aspergillosis (6), CARD9 may mediate organ-specific effector function of recruited and/or tissue-resident mononuclear phagocytes that may contribute to the extrapulmonary tissue tropism of the aspergillosis seen in CARD9-deficient patients. Thus, future work will be required to examine whether and

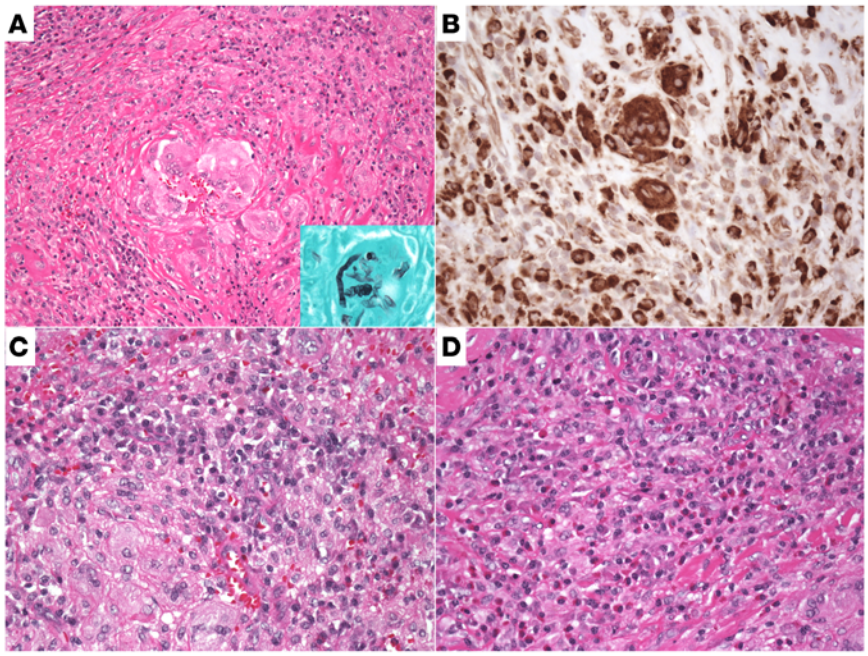

Figure 6. Caspase recruitment domain family member 9 (CARD9) deficiency is associated with impaired neutrophil accumulation in the extrapulmonary infected tissue. Biopsy of this suprarenal mass shows areas of palisading inflammation, in which giant cells/histiocytes (**A**) engulf *Aspergillus* hyphae (inset) and are CD68$^+$ by immunohistochemistry (**B**). Surrounding the histiocytic infiltration are sheaths of plasma cells (**C**) and eosinophils (**D**). No neutrophils are seen. Magnification, ×200 (**A**); ×400 (**A** inset and **B**–**D**).

by which mechanisms CARD9 deficiency may adversely affect inflammatory and patrolling monocyte, macrophage, and dendritic cell innate immune responses against *Aspergillus* in mice and humans.

In summary, we report that CARD9 deficiency results in aspergillosis that involves extrapulmonary tissues, associated with an inability to mobilize neutrophils to the site of infection without neutrophil-intrinsic chemotactic or anti-*Aspergillus* effector function deficits. Investigation of a larger number of CARD9-deficient patients and mouse mechanistic studies will help better understand the molecular and cellular bases of organ-specific innate immune responses against *Aspergillus* and verify the strictly extrapulmonary tropism of aspergillosis observed in our CARD9-deficient patients. Importantly, clinicians should be aware that patients who develop invasive mold disease without known immunosuppression merit evaluation for CARD9 deficiency, especially when extrapulmonary sites are involved.

Methods

Study participants. Patients with aspergillosis and healthy donors provided written informed consent for participation in the study (see Study approval section below). For healthy donor enrollment, a prescreening questionnaire along with a pre-donation assessment was performed to select individuals with no known lung, heart, kidney, or bleeding disorders, and without history of injection drug use or high-risk activities predisposing to HIV infection.

CARD9 genotyping. Verification of the *CARD9* mutation found by WES in patient 1 was performed using Sanger sequencing. In brief, PCR reactions were performed in a total volume of 25 μl of a solution containing 10 ng genomic DNA, 12.5 μl Go-Taq Colorless Master-Mix (Promega), and 1 μl forward and reverse primer (each 5 pmol, Eurofins MWG Operon). Thermal cycling was performed on the GeneAMP PCR System 9700 (Applied Biosystems) using the following cycling conditions: 95°C for 2 minutes, 35 cycles of 95°C for 10 seconds, 63°C for 20 seconds, and 72°C for 25 seconds, with a final 5-minute extension at 72°C. Primers for this PCR were 5′-GAGCTGCAGCAGGAGAAGG-3′ (forward) and 5′-AGGAGTGGGTGAGTGGAGG-3′ (reverse). A region of 422 bp was amplified and genotyping was performed using RFLP analysis. For this purpose, 1 μg of PCR product was digested at 37°C overnight with 5 U BfaI (restriction site: CTAG) in a 10-μl reaction mix containing 1 μl CutSmart Buffer (both from NEB). Digested products were run in a 1.5% agarose gel, stained with GelRed Nucleic Acid Stain (Biotium), and visualized using a UV transilluminator. For DNA sequencing, PCR products were purified using a QIAquick PCR Purification Kit according to the instructions of the manufacturer (QIAGEN). Finally, 5 ng/μl, in a total volume of 15 μl, was sent together with 2 pmol/μl primers to Eurofins MWG Operon for further sequencing analysis.

For targeted *CARD9* sequencing in patient 2, DNA was harvested from whole blood using the Gentra Puregene Blood DNA isolation Kit (QIAGEN) per the manufacturer's instructions. Genomic amplification was performed in 15-μl reactions using Platinum PCR SuperMix High Fidelity (Life Technologies), 0.625 mM of each primer, and 10–200 ng of DNA. Cycling conditions were 95°C for 3 minutes followed by 35 cycles of 95°C for 20 seconds, and 68°C for 2 minutes and 45 seconds. PCR products were purified

using ExoSAP-IT (USB products by Affymetrix), sequenced using Big Dye Terminators v3.1 (Life Technologies), cleaned up using Performa DTR Ultra spin plates, and run on an ABI 3730XL. Amplification and sequencing primers are shown in Supplemental Table 1.

Histology. Human tissues were fixed with 10% formalin and paraffin embedded. Tissue sections were deparaffinized and stained with H&E or Grocott-Gomori's methenamine silver (GMS). In addition, CD68 immunostaining was performed in human tissue using monoclonal antibody CONFIRM CD68 (KP-1) from Ventana (Roche, catalog 790-2931). Detection was done on an automated system using Ultra-View DAB on a Bench mark ULTRA from Ventana (Roche) according to the manufacturer's instructions. Images were taken using an Olympus BX41 microscope, objectives UPlanFL 10×/030, 20×/0.50 ∞/0.17, 40×/0.75 ∞/0.17 with the adaptor U-TV0.5xC using the digital camera Q-imaging Micropublisher 5.0 RTV. The images were captured using Q-Capture Version 3.1 and imported into Adobe Photoshop 7.0.

Isolation of human PBMCs and neutrophils from peripheral blood. PBMCs were harvested from whole blood by gradient centrifugation using Percoll (patient 1) or Lymphocyte Separation Media (Lonza) (patient 2) and used in stimulation assays. Neutrophils were isolated using 3% dextran in 0.85% sodium chloride and red blood cells lysed using sequential exposure to 0.2% and 1.6% NaCl solutions. Neutrophils (>95% pure and viable) were used in functional assays of conidial internalization, inhibition of conidial germination, oxidative burst, fungal killing, and chemotaxis (34).

PBMC stimulation and cytokine determination by ELISA or Luminex array. To determine whether the patients' PBMCs had impaired ability to produce proinflammatory cytokines, ELISA (patient 1) or a Luminex-based assay (patient 2) was used. In brief, PBMCs from healthy donors or the CARD9-deficient patients were incubated in duplicate in a round-bottom 96-well plate (Corning Inc.) at 37°C in a 5% CO_2 incubator in RPMI 1640 containing 10% FBS (Gibco), 100 U/ml penicillin, and 100 μg/ml streptomycin (unstimulated). Stimulated PBMCs were incubated in RPMI 1640 plus 10% FBS/antibiotics containing LPS (100 ng/ml), live (2.5×10^5 ml; patient 1) or heat-killed *C. albicans* SC5314 (1×10^6/ml; patient 2), or heat-killed *A. fumigatus* B-5233 conidia (1×10^8/ml; patient 2) or live *S. aureus* 502A (2×10^6/ml). After 24 or 48 hours of stimulation, PBMCs were pelleted and the supernatant was collected and stored at –80°C until analysis. For patient 1, the concentrations of IL-1β and IL-6 were measured using Pelikine ELISA (Sanquin Reagents) according to the manufacturer's recommendations. For patient 2, Luminex analysis for IL-1α, IL-1β, IL-6, GM-CSF, IFN-γ, and TNF-α was performed via a multiplex bead array assay with antibodies and cytokine standards to generate known-concentration curves (R&D Systems, Peprotech). Individual Luminex bead sets (Luminex) were coupled to cytokine-specific capture antibodies according to the manufacturer's protocols and biotinylated polyclonal antibodies were used at twice the recommended concentrations for a classical ELISA according to the manufacturer's instructions. The assay was run with 1,200 beads per set of cytokines in a volume of 50 μl. The plates were read on a Luminex MAGPIX platform where more than 50 beads were collected per bead set. The median fluorescence intensity of the beads was then measured for each individual bead, which was analyzed with the Millipex software using a 5P regression algorithm.

A. fumigatus strains. Two clinical strains of *A. fumigatus* obtained from patients with invasive pulmonary aspergillosis were used for neutrophil functional assays in patient 1 (Sq-001) and 2 (B-5233, ref. 35). The mutant B-5233/GFP was also used for neutrophil functional assays in patient 2. The strains were maintained as previously described (36). The *A. fumigatus* B-5233/GFP strain was generated by transforming B-5233 with a plasmid to express GFP under oxidative stress. The transforming plasmid was constructed by inserting the sGFP gene from the vector p/DV2 (37) in frame with the AFUA_5g12770 ORF, before its termination codon. Thus, transcription of GFP is regulated by the promoter of AFUA_5g12770, which encodes a metallo-β-lactamase-family protein. The AFUA_5g12770 gene is highly upregulated in *A. fumigatus* exposed to neutrophils capable of producing ROS but not to neutrophils deficient in ROS production (38).

Neutrophil phagocytosis of Aspergillus conidia. Phagocytosis of serum-opsonized *Aspergillus* conidia by control and CARD9-deficient neutrophils of patient 1 was assessed by flow cytometry. During the incubation of neutrophils with FITC-labeled conidia of *A. fumigatus* Sq-001, a sample was obtained and tested every 5 to 10 minutes for up to 90 minutes at 37°C using a LSRII flow cytometer equipped with FACSDiva software (BD Biosciences). Neutrophils were gated based on their forward and side scatter, and 10,000 gated events were collected per sample. Based on the percentage of FITC-positive neutrophils, phagocytosis was calculated relative to control neutrophils.

Prevention of conidial germination and killing of Aspergillus conidia and hyphae by neutrophils using MTT. For assessing the antifungal activity of neutrophils from patient 1, *A. fumigatus* Sq-001 was opsonized with 10% v/v pooled serum or IgGs (15 mg/ml, IVIG, Nanogam, Sanquin) for 15 minutes, at 37°C. Complement inactivation of the pooled serum was performed by heat treatment at 56°C for 30 minutes.

For assessing neutrophil-mediated prevention of conidial germination, *Aspergillus* conidia were incubated overnight with neutrophils from patient 1 (0–5 × 10^6 neutrophils/ml; effector/target ratio, 1:2,000 to 1:100) in a 96-well plate at 37°C in RPMI 1640 medium containing L-glutamine and 10% FCS (Life Technologies). Subsequently, the neutrophils were lysed in water/NaOH (pH 11.0) and incubated with MTT (Sigma-Aldrich). After addition of acidic isopropanol (0.04 M HCl) the optical density was measured in a plate reader at 570 nm (Tecan) and the *A. fumigatus* hyphae viability was calculated as compared with that of hyphae incubated without neutrophils (set at 100%). To assess the *A. fumigatus* hyphae killing by neutrophils, conidia were incubated overnight at 37°C in RPMI 1640 medium containing L-glutamine and 10% FCS upon formation of a monolayer as determined by microscopy. Freshly isolated neutrophils from patient 1 (5.0 × 10^6 cells/ml) were cultured for 1 hour on the preformed *A. fumigatus* monolayer at 37°C. Thereafter, the cells were lysed in water/NaOH (pH 11.0) and incubated with MTT. The absorbance of the acidic isopropanol–diluted samples was measured on the plate reader and the viability was calculated as a percentage of the viability after incubation without neutrophils.

Conidial and hyphal neutrophil killing assays by XTT. To assess the neutrophil killing capacity of patient 2, freshly harvested conidia of *A. fumigatus* B-5233 were suspended in R25 (RPMI 1640 supplemented with 25 mM Hepes) at concentrations of 3.33 × 10^5 and 3.33 × 10^6 conidia/ml, for conidial and hyphal assays, respectively. The conidial suspension (300 μl) was added to the wells of a 24-well plate, and the plates were kept at 4°C for approximately 20 hours. Two hours prior to adding neutrophils from patient 2, plates were transferred to 37°C and 5% CO_2. One hundred microliters of R25 containing 1 × 10^5 neutrophils (conidial assay) or 1 × 10^6 neutrophils (hyphal assay) and 20 μl of plasma were added to each well, except for the control wells, which received only plasma in R25. Plates were incubated at 37°C for 18 hours (conidial assay) or 2 hours (hyphal assay) before neutrophils were lysed. To lyse neutrophils, 400 μl of 1.25% of Triton-X 100 (Sigma-Aldrich) was added to the wells. Wells were then washed 3 times with PBS. Neutrophil-mediated growth inhibition of fungal cells was determined by changes in metabolic activity measured by the XTT (2,3-bis-(2-methoxy-4-nitro-5-sulfophenyl)-2H-tetrazolium-5-carboxanilide) assay (39) as follows: 200 μl Dulbecco's PBS containing 0.5 mg/ml XTT (Sigma-Aldrich, X4626) and 40 μg/ml coenzyme Q (Sigma-Aldrich, D9150) were added to the wells. Plates were incubated at 37°C for 1 hour before supernatants were filtered through a MultiScreen HTS 96-well filtration system (EMD Millipore) and absorbance was read at 450 nm. In addition to the plates containing plasma (opsonized), plates without plasma (nonopsonized) were also analyzed following the protocol described above except for the absence of plasma.

NADPH oxidase activity of neutrophils. NADPH oxidase activity was assessed as the release of H_2O_2, determined by the Amplex Red method (Molecular Probes) by neutrophils from patient 1 treated with various stimuli: zymosan (1 mg/ml); serum-treated zymosan (STZ, 1 mg/ml); phorbol-12-myristate-13-acetate (PMA, 100 ng/ml); PAF followed by formyl-Met-Leu-Phe (fMLP); *Candida* particles (ratio with neutrophils, 1:4); and aggregated IgG (5 mg/ml); in the presence of Amplex Red (0.5 μM) and horseradish peroxidase (1 U/ml). Fluorescence was measured at 30-second intervals for 20 minutes with the HTS7000plus plate reader (Tecan). Maximal slope of H_2O_2 release was assessed over a 2-minute interval (34).

Assessment of neutrophil-induced oxidative damage in Aspergillus. The induction of neutrophil ROS during interaction with *A. fumigatus* was visualized with the aid of the B-5233/GFP strain, which expresses GFP under oxidative stress. Images of the interaction between neutrophils from patient 2 and germinated conidia were obtained using 8-well chamber slides (Thermo Fisher Scientific). Three hundred microliters of 3.33 × 10^5 conidia/ml was added to each well of the chamber slide, and the slide was kept at 4°C for approximately 20 hours. Four hours prior to exposure of germinated conidia to neutrophils, the slide was transferred to 37°C. At the end of 4 hours, 100 μl R25 containing 1 × 10^5 neutrophils and 20 μl plasma were added to the wells. Control wells received either 100 μl R25 alone or R25 with 375 μM H_2O_2. Slides were incubated at 37°C for 4 hours before microscopy (Zeiss Inverted Microscope, Axiovision 4 software). All images were taken with the same exposure time.

Neutrophil chemotaxis. Neutrophils (5 × 10^6/ml) from patient 1, another CARD9-deficient patient with the c.883C>T (p.Q295X) mutation, and from 2 healthy donors were incubated with calcein-AM (final concentration, 1 μM; Molecular Probes) for 30 minutes at 37°C, washed twice, and resuspended in Hepes buffer

at a concentration of 2×10^6/ml. FluoroBlok chemotaxis was measured using 3-μm pore-size FluoroBlock inserts (Corning Inc.) in a Falcon 24-well plate. Calcein-labeled PMNs (2×10^6/ml, 0.3 ml) were pipetted in the insert (upper compartment), and placed in the lower compartment containing 0.8 ml C5a (10^{-8} M), IL-8 (10^{-8} M), or PAF (10^{-7} M). Fluorescence was measured underneath the filter every 2.5 minutes for 45 minutes with a Tecan Infinite F200-pro plate reader at an excitation wavelength of 485 nm and an emission wavelength of 535 nm.

Immunoblot analyses. Analysis of CARD9 protein expression was performed by Western blot analysis in PBMCs from patients 1 and 2 and healthy donors. For patient 1, the following antibodies were used for detection as previously described (19): CARD9 (Proteintech Group, catalog 10669-1-AP, 1:400) and GAPDH (Merck Millipore, catalog MAB374, 1:1,000). For patient 2, PBMCs from 2 healthy donors and the patient were lysed in RIPA lysis buffer (10 mM Tris-HCl, 140 mM NaCl, 1 mM EDTA, 0.5 mM EGTA, 1% Triton X-100, 0.1% sodium deoxycholate, 0.1% SDS) supplemented with protease inhibitors (Halt Protease and Phosphatase Inhibitor Cocktail; Thermo Fisher Scientific, catalog 1861281). Equal amounts of proteins were resolved by SDS-PAGE and transferred onto an Immobilon P polyvinylidene difluoride membrane (EMD Millipore). The membranes were then incubated with the following antibodies: CARD9 (Proteintech Group, catalog 10669-1-AP, 1:400) and GAPDH (Cell Signaling Technology, catalog 5174S, 1:2,000). HRP-conjugated secondary antibodies were from Southern Biotech. The antigens were visualized using the Immobilon Western Chemiluminescent HRP substrate (EMD Millipore) according to the manufacturer's instructions.

Determination of IL-17A$^+$CD4$^+$ T cells. PBMCs from our CARD9-deficient patients were isolated as described above and cultured in RPMI 1640 with 10% FBS, 2 mM L-glutamine, 100 U/ml penicillin, and 100 μg/ml streptomycin (Gibco) at 37°C in a humidified 5% CO_2 incubator. Intracellular staining for IL-17A was performed on PBMCs stimulated with PMA and ionomycin as previously described (14). After surface staining with anti-CD4 (clone PA-T4, eBioscience), cells were washed, fixed, permeabilized, incubated with anti-IL-17A (clone eBio64CAP17, eBioscience), and acquired on a FACSCanto (BD Biosciences).

Statistics. The experimental data were analyzed using 2-tailed unpaired *t* test or Mann-Whitney test with GraphPad Prism 6.0 and presented as mean ± SEM. Statistical significance was defined as $P < 0.05$.

Study approval. Patients with aspergillosis and healthy donors were enrolled in protocols approved by the NIAID and National Cancer Institute IRB committees at the NIH and by the IRB committees of the University of Tübingen and the University of Amsterdam, and provided written informed consent for study participation. The study was conducted in accordance with the Helsinki Declaration.

Author contributions

NR, RPG, AFF, and MSL wrote the manuscript. NR, RPG, AFF, APH, ALC, JAS, KJKC, TWK, and MSL designed the research studies. NR, AFF, CR, VKP, KWW, SMH, DH, and MSL evaluated patients and provided patient care and coordinated the conduct of clinical research studies. NR, RPG, APH, ALC, JAS, RAD, KH, CH, LC, MM, MS, ME, RS, BN, FE, CMM, SP, AS, JDM, and JKL conducted experiments. NR, RPG, APH, ALC, JAS, RAD, KH, MM, MS, ME, RS, BN, FE, CMM, SP, AS, JDM, and JKL acquired data. NR, RPG, APH, ALC, JAS, KH, CMM, SP, JDM, JKL, KJKC, TWK, and MSL analyzed data.

Acknowledgments

The authors thank the patients and their families for their participation in our study and dedicate this report to our patient N. A., who succumbed to invasive aspergillosis at the age of 12, and to his family.

This work was supported by the Division of intramural Research (DIR), NIAID, NIH, the Landsteiner Foundation for Blood Transfusion Research (LSBR 1706), the German Center for Infection Research (DZIF), and the German Research Foundation (DFG). The funding sources had no involvement in the study design, in the collection, analysis and interpretation of data, in the writing of the report, or in the decision to submit the article for publication.

Address correspondence to: Michail S. Lionakis, 9000 Rockville Pike, Building 10/Room 11C102, Bethesda, Maryland, 20892, USA. Phone: 301.443.5089; E-mail: lionakism@mail.nih.gov. Or to: Taco W. Kuijpers, Immunology and Infectious Diseases, Emma Children's Hospital, Academic Medical Center (AMC),

Location H7 – 230, Meibergdreef 9, 1105 AZ Amsterdam, The Netherlands. Phone: 31.20.566.2727; E-mail: t.w.kuijpers@amc.uva.nl. Or to: Dominik Hartl, Department of Pediatrics I, Infectious Diseases & Immunology, University of Tübingen, Ebene C4 / Raum 305, Hoppe-Seyler-Strasse 1Building, 72076 Tübingen, Germany. Phone: 49.7071.29.81460; E-mail: Dominik.Hartl@med.uni-tuebingen.de.

FE's present address is: Institute for Infectious Diseases and Zoonoses, Ludwig-Maximilians-University, Munich, Germany.

1. Garcia-Vidal C, Viasus D, Carratalà J. Pathogenesis of invasive fungal infections. *Curr Opin Infect Dis*. 2013;26(3):270–276.
2. Brown GD, Denning DW, Gow NA, Levitz SM, Netea MG, White TC. Hidden killers: human fungal infections. *Sci Transl Med*. 2012;4(165):165rv13.
3. Segal BH. Aspergillosis. *N Engl J Med*. 2009;360(18):1870–1884.
4. Lionakis MS, Netea MG, Holland SM. Mendelian genetics of human susceptibility to fungal infection. *Cold Spring Harb Perspect Med*. 2014;4(6).
5. Spinner MA, et al. GATA2 deficiency: a protean disorder of hematopoiesis, lymphatics, and immunity. *Blood*. 2014;123(6):809–821.
6. Lanternier F, et al. Primary immunodeficiencies underlying fungal infections. *Curr Opin Pediatr*. 2013;25(6):736–747.
7. Netea MG, et al. Immune sensing of Candida albicans requires cooperative recognition of mannans and glucans by lectin and Toll-like receptors. *J Clin Invest*. 2006;116(6):1642–1650.
8. Drummond RA, Brown GD. Signalling C-type lectins in antimicrobial immunity. *PLoS Pathog*. 2013;9(7):e1003417.
9. Gazendam RP, et al. Two independent killing mechanisms of Candida albicans by human neutrophils: evidence from innate immunity defects. *Blood*. 2014;124(4):590–597.
10. Picard C, Casanova JL, Puel A. Infectious diseases in patients with IRAK-4, MyD88, NEMO, or IκBα deficiency. *Clin Microbiol Rev*. 2011;24(3):490–497.
11. Robinson MJ, Sancho D, Slack EC, LeibundGut-Landmann S, Reis e Sousa C. Myeloid C-type lectins in innate immunity. *Nat Immunol*. 2006;7(12):1258–1265.
12. Glocker EO, et al. A homozygous CARD9 mutation in a family with susceptibility to fungal infections. *N Engl J Med*. 2009;361(18):1727–1735.
13. Lanternier F, et al. Inherited CARD9 deficiency in otherwise healthy children and adults with Candida species-induced meningoencephalitis, colitis, or both. *J Allergy Clin Immunol*. 2015;135(6):1558–68.e2.
14. Drummond RA, et al. CARD9-dependent neutrophil recruitment protects against fungal invasion of the central nervous system. *PLoS Pathog*. 2015;11(12):e1005293.
15. Lanternier F, et al. Deep dermatophytosis and inherited CARD9 deficiency. *N Engl J Med*. 2013;369(18):1704–1714.
16. Liang P, Wang X, Wang R, Wan Z, Han W, Li R. CARD9 deficiencies linked to impaired neutrophil functions against Phialophora verrucosa. *Mycopathologia*. 2015;179(5-6):347–357.
17. Lanternier F, et al. Inherited CARD9 deficiency in 2 unrelated patients with invasive Exophiala infection. *J Infect Dis*. 2015;211(8):1241–1250.
18. Gross O, et al. Card9 controls a non-TLR signalling pathway for innate anti-fungal immunity. *Nature*. 2006;442(7103):651–656.
19. Drewniak A, et al. Invasive fungal infection and impaired neutrophil killing in human CARD9 deficiency. *Blood*. 2013;121(13):2385–2392.
20. Rieber N, et al. Pathogenic fungi regulate immunity by inducing neutrophilic myeloid-derived suppressor cells. *Cell Host Microbe*. 2015;17(4):507–514.
21. Svenson IK, et al. Identification and expression analysis of spastin gene mutations in hereditary spastic paraplegia. *Am J Hum Genet*. 2001;68(5):1077–1085.
22. Adzhubei IA, et al. A method and server for predicting damaging missense mutations. *Nat Methods*. 2010;7(4):248–249.
23. Kircher M, Witten DM, Jain P, O'Roak BJ, Cooper GM, Shendure J. A general framework for estimating the relative pathogenicity of human genetic variants. *Nat Genet*. 2014;46(3):310–315.
24. Gavino C, et al. Impaired RASGRF1/ERK-mediated GM-CSF response characterizes CARD9 deficiency in French-Canadians. *J Allergy Clin Immunol*. 2016;137(4):1178–88.e1.
25. Herbst M, et al. Chronic Candida albicans meningitis in a 4-year-old girl with a homozygous mutation in the CARD9 gene (Q295X). *Pediatr Infect Dis J*. 2015;34(9):999–1002.
26. Cramer RA, Rivera A, Hohl TM. Immune responses against Aspergillus fumigatus: what have we learned? *Curr Opin Infect Dis*. 2011;24(4):315–322.
27. Latgé JP. Aspergillus fumigatus and aspergillosis. *Clin Microbiol Rev*. 1999;12(2):310–350.
28. Jhingran A, et al. Compartment-specific and sequential role of MyD88 and CARD9 in chemokine induction and innate defense during respiratory fungal infection. *PLoS Pathog*. 2015;11(1):e1004589.
29. Drummond RA, Lionakis MS. Mechanistic insights into the role of C-type lectin receptor/CARD9 signaling in human antifungal immunity. *Front Cell Infect Microbiol*. 2016;6:39.
30. Berenguer J, et al. Pathogenesis of pulmonary aspergillosis. Granulocytopenia versus cyclosporine and methylprednisolone-induced immunosuppression. *Am J Respir Crit Care Med*. 1995;152(3):1079–1086.
31. Lionakis MS, Kontoyiannis DP. Glucocorticoids and invasive fungal infections. *Lancet*. 2003;362(9398):1828–1838.
32. Wang X, et al. CARD9 mutations linked to subcutaneous phaeohyphomycosis and TH17 cell deficiencies. *J Allergy Clin Immunol*. 2014;133(3):905–908.e3.
33. Caffrey AK, et al. IL-1α signaling is critical for leukocyte recruitment after pulmonary Aspergillus fumigatus challenge. *PLoS Pathog*. 2015;11(1):e1004625.

34. Drewniak A, Tool AT, Geissler J, van Bruggen R, van den Berg TK, Kuijpers TW. Toll-like receptor-induced reactivity and strongly potentiated IL-8 production in granulocytes mobilized for transfusion purposes. *Blood*. 2010;115(22):4588–4596.
35. Sugui JA, et al. Role of laeA in the regulation of alb1, gliP, conidial morphology, and virulence in Aspergillus fumigatus. *Eukaryotic Cell*. 2007;6(9):1552–1561.
36. Tsai HF, Chang YC, Washburn RG, Wheeler MH, Kwon-Chung KJ. The developmentally regulated alb1 gene of Aspergillus fumigatus: its role in modulation of conidial morphology and virulence. *J Bacteriol*. 1998;180(12):3031–3038.
37. McCluskey K. The Fungal Genetics Stock Center: from molds to molecules. *Adv Appl Microbiol*. 2003;52:245–262.
38. Sugui JA, et al. Genes differentially expressed in conidia and hyphae of Aspergillus fumigatus upon exposure to human neutrophils. *PLoS One*. 2008;3(7):e2655.
39. Meshulam T, Levitz SM, Christin L, Diamond RD. A simplified new assay for assessment of fungal cell damage with the tetrazolium dye, (2,3)-bis-(2-methoxy-4-nitro-5-sulphenyl)-(2H)-tetrazolium-5-carboxanil ide (XTT). *J Infect Dis*. 1995;172(4):1153–1156.